

X-ray signature of antistars in the Galaxy

A.E. Bondar,^{a,e} S.I. Blinnikov,^{b,c} A.M. Bykov,^d A.D. Dolgov,^e
K.A. Postnov^{c,e,1}

^aBudker INP, Lavrentieva 11, Novosibirsk, 630090, Russia

^bNRC “Kurchatov institute” - ITEP, B. Cheremushkinskaya 25, 117218, Moscow, Russia

^cSternberg Astronomical Institute, M.V. Lomonosov Moscow State University,
13, Universitetskij pr., 119234, Moscow, Russia

^dIoffe Institute, Politechnicheskaya 26, St Petersburg

^eDepartment of Physics, Novosibirsk State University,
Pirogova 2, 630090, Novosibirsk, Russia

E-mail: pk@sai.msu.ru, byk@astro.ioffe.ru, dolgov@fe.infn.it, sergei.blinnikov@itep.ru

Abstract. The existence of macroscopic objects from antimatter (antistars) is envisaged in some models of baryogenesis. Searches for antistars have been usually carried out in gamma-rays originated from hadronic annihilation of matter. In astrophysically plausible cases of the interaction of neutral atmospheres or winds from antistars with ionized interstellar gas, the formation of excited $p\bar{p}$ and $\text{He}\bar{p}$ atoms precedes the hadronic annihilation. These atoms rapidly cascade down to low levels before annihilation giving rise to a series of narrow lines which can be associated with the hadronic annihilation gamma-ray emission. The most significant are L (3p-2p) 1.73 keV line (yield more than 90%) from $p\bar{p}$ atoms, and M (4-3) 4.86 keV (yield $\sim 60\%$) and L (3-2) 11.13 keV (yield about 25%) lines from $^4\text{He}\bar{p}$ atoms. These lines can be searched for in dedicated observations by the forthcoming sensitive X-ray spectroscopic missions XRISM, *Athena* and *Lynx* and in wide-field X-ray surveys like SRG/*eROSITA* all-sky survey.

¹Corresponding author.

Contents

1	Introduction	1
2	Line emissions from protonium decays	2
3	keV X-ray emission from protonium cascades in Galactic antistar candidates	4
4	Associated e^+e^- emission and optical lines	5
5	Helium-antiproton and antihelium-proton cascade X-ray lines from antistars	6
6	Possible astrophysical sources	7
7	Constraints from electron-positron annihilations	9
8	Conclusions	10

1 Introduction

According to the accepted conviction, the universe in our neighborhood consists solely of matter, and the existence of macroscopically large antimatter objects is fully excluded. This is in accordance with the conventional picture that the excess of baryons over antibaryons in the Universe is generated by Sakharov's mechanism [1]. In models with explicit C and CP violation, the baryon asymmetry

$$\eta = (N_B - N_{\bar{B}})/N_\gamma \approx 6 \cdot 10^{-10} \quad (1.1)$$

is a universal constant over the whole universe. Here $N_{B(\bar{B})}$ are the number densities of baryons or antibaryons, and $N_\gamma = 411/\text{cm}^3$ is the current number density of photons in the cosmic microwave background (CMB) radiation.

If the charge symmetry is broken spontaneously, then domains of matter and antimatter may exist but the size of domains is expected to be cosmologically large, at the Gigaparsec level [2]. Therefore, the accepted faith is that if even macroscopically large objects or regions consisting of antimatter exist, they should be far away from us at the edge of the universe or at least at distances beyond 10 Mpc [3].

On the other hand, about a quarter of a century ago, a physical mechanism was suggested leading to the possible formation of compact antistars over normal matter-dominated background [4, 5]. According to the proposed scenario, the baryogenesis in the bulk of the universe proceeded in the usual way giving rise to the observed small baryon asymmetry (1.1), while in a small by volume part of the universe, bubbles with a very high baryonic number (called HBB) might be created. The model allows for the formation of HBBs with both signs of the baryon asymmetry, positive (matter) and negative (antimatter). HBBs with a size comparable to the cosmological horizon at the QCD (quantum chromodynamics) phase transition at $T \sim 100$ MeV mostly give rise to primordial black holes (PBHs) which could make a sizeable fraction (if not all) of cosmological dark matter. Such PBHs could have masses in a wide range from a fraction to thousands of solar masses [6, 7]. Of course, there is no noticeable difference between a PBH and an anti-PBH.

Smaller HBBs could form compact stars or antistars. They would be created in the very early universe after the QCD phase transition at $T \sim 100$ MeV. Probably, they can be now observed as

peculiar stars in the Galaxy: too old stars, very fast-moving stars, and stars with a highly unusual chemical content [8–10], for a review see [11]. They should also populate the galactic halo. The fraction of these strange stars and/or antistars among the stellar population is model-dependent but may be quite high.

The possibility of the existence of a population of antistars in the Galaxy and observational limits on their density were analyzed in several papers [12–15]. It was concluded that quite a noticeable fraction of antistars relative to ordinary stars is not excluded by the present observations. As discussed in detail in ref. [15], the restrictive limits derived for the “normal” antistars from gamma-ray background (e.g. [16]) are not applicable for antistars produced in scenarios [4]–[14], and such antimatter objects may abundantly populate the Galaxy without contradicting the gamma-ray background limits.

Recently, the idea that antistars may be our Galactic neighbors attracted new attention. In ref. [17], it was suggested that cosmological dark matter could entirely consist of macroscopic antimatter objects and in ref. [18] a possible indication to antistars in the Galaxy based on gamma-ray *Fermi*/LAT measurements was reported. Quoting the latter paper: “We identify in the catalog 14 antistar candidates not associated with any objects belonging to established gamma-ray source classes and with a spectrum compatible with baryon-antibaryon annihilation.”

In this paper, we propose a new signature tagging electromagnetic signal from annihilation in outer layers of antistars. The idea is to search for antistars in the Galaxy through X-rays in the $\sim (1 - 10)$ keV energy band. This X-ray radiation is expected to be produced in the process of the cascade transition from bound states of antiproton-proton (protonium) or antihelium-proton atoms before $p\bar{p}$ -annihilation and must accompany the gamma-ray radiation from the annihilation.

Note that the *Fermi* candidate antistars are not true stars but large regions in the sky plane (of order tens angular minutes in diameter corresponding to *Fermi*/LAT gamma-ray error boxes) comprising a huge number of stars. Obviously, not only antistars but also objects consisting of ordinary matter can be sources of gamma-quanta with energies above 100 MeV. Therefore, the objects showing the X-ray signature proposed in our paper will lead to an unambiguous indication of their antimatter nature and much better localization if they are detected in future observations.

2 Line emissions from protonium decays

Usually, the antimatter objects are being looked for through the search for energetic photons with energies of hundreds MeV from π^0 decays into two γ -quanta, with π^0 emerging from $p\bar{p}$ -annihilation. The energy spectrum of such photons is shown in Fig. 1. This spectrum was calculated by Geant4¹ [19] simulation of the low-energy antiproton annihilation in a small liquid hydrogen target. The spectrum suggests that the mean energy radiated in gamma-rays per one annihilation is $\Delta E_\gamma = 617.5$ MeV. The mean number of γ -quanta per one annihilation is $\langle N_\gamma \rangle = 4.12$ with the mean number of γ -quanta above 100 MeV is $\langle N_\gamma \rangle(> 100\text{MeV}) = 2.63$ per event. Note that the target’s material and structure do not significantly affect the annihilation spectrum which is appropriate for the considered problem.

However, before annihilation, protons and antiprotons could form atomic-type excited bound states (‘protonium’, Pn), similar to e^+e^- -positronium (Ps) atoms. One could expect that in the process of de-excitation of Pn, an antistar could emit not only ~ 100 -MeV gamma-rays but a noticeable flux of X-rays with energies in the keV range.

Let us briefly remind the basic physics of $p\bar{p}$ annihilation through a protonium state (see, e.g, [20] for a comprehensive review). A protonium atom can form during the interaction of a p with

¹version Geant4.10.06 (06.12.2019); <https://geant4.web.cern.ch>

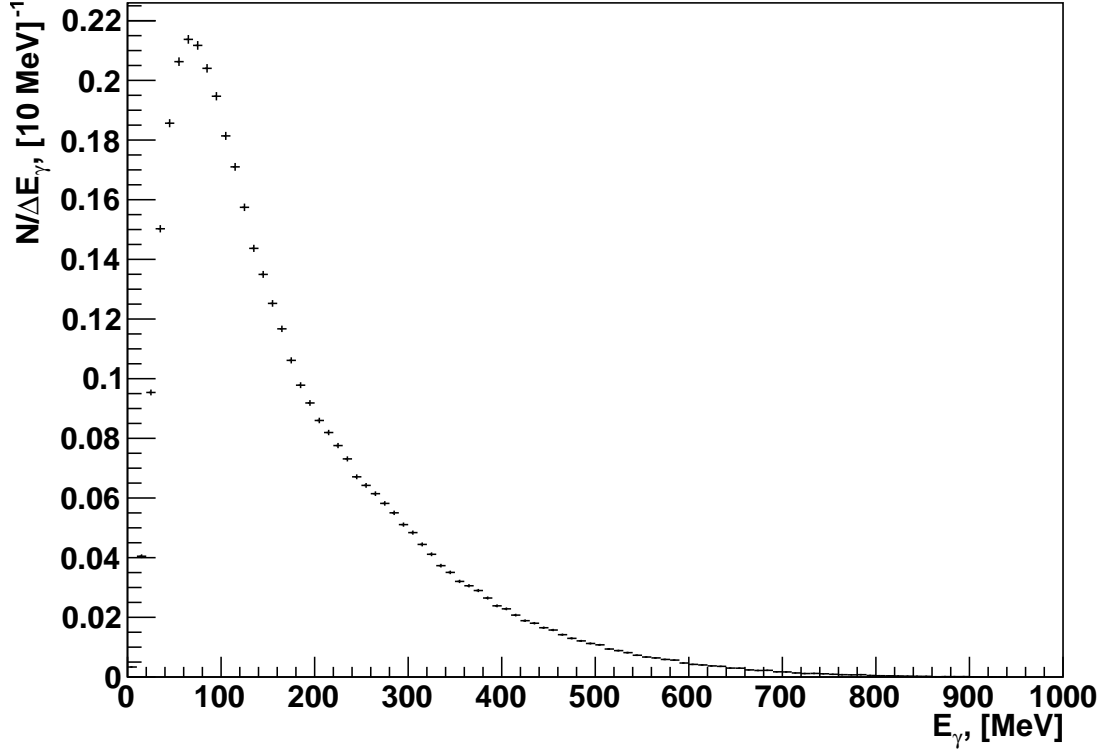


Figure 1. Gamma-ray spectrum from hadronic $p\bar{H}$ annihilation. The mean number of γ -quanta per event is $\langle N_\gamma \rangle = 4.12$. The mean number of γ -quanta above 100 MeV is 2.63 per event. The mean energy radiated in gamma-rays per one annihilation is $\Delta E_\gamma = 617.5$ MeV. Calculations by Geant4 code.

neutral (or molecular) antimatter. In the ionized matter-antimatter interaction, the annihilation mainly proceeds through the direct hadronic channel, the cross-section of the radiative recombination of a Pn atom formation from the $p\bar{p}$ interaction being $(m_e/m_p)^{3/2} \approx 10^{-5}$ times smaller (see [3] for the matter-antimatter annihilation cross-sections).

A Pn atom forms when a proton (antiproton) interacts with an anti-hydrogen (hydrogen) atom, $\bar{p} + H \rightarrow (p, \bar{p}) + e^-$. The formation of a Pn atom effectively occurs when the energy of the proton in the lab frame is below the electron's ionization threshold in atomic hydrogen, $E = 1\text{Ry} \approx 13.6$ eV. At lower proton energies, the cross-section increases as $\sim 1/\sqrt{E}$ [21]. Therefore, in the present paper, we will mainly focus on astrophysical situations where the antistar's atmosphere (or its stellar wind) is neutral or interacts with the neutral interstellar medium (ISM).

The fraction of energy from the bolometric luminosity released in X-ray from the Pn cascades (the cascade yield), $f_X = L_X(Pn)/L_a$, depends on the pressure [22]. However, an upper limit on the bolometric X-ray yield per unit cascade can be estimated as the binding energy of a Pn atom, ≈ 12.5 keV (ignoring small QED corrections $O(\alpha^2)$). Therefore, the maximum X-ray yield per one Pn atom is $R_{p\bar{p}} = (1/4)\alpha^2 m_p c^2 = 12.5$ keV (α is the fine structure constant, m_p is proton's mass). As the cascade time of a Pn atom is very short [22], in rarefied media the X-ray luminosity in X-ray lines will be determined by the formation rate of Pn atoms, \dot{N}_a : $L_X \leq 12.5 \text{ keV} \times \dot{N}_a$, i.e. the maximum possible X-ray fraction in the Pn-cascade during matter-antimatter annihilation is $f_{X,\text{max}} = \alpha^2/8 \approx 6.7 \times 10^{-6}$.

The line energies for the K (Lyman) $2p \rightarrow 1s$, L (Balmer) $3d \rightarrow 2p$ and M (Paschen) $4f \rightarrow 3d$ transitions in a Pn atom are 9409 eV, 1737 eV and 607 eV, respectively. Calculations of the X-ray line yields from the Pn decays produced in $p\bar{H}$ interactions at low densities [23] suggest that most intensive X-ray lines should be Balmer (L) lines (up to 97%), the 2p-states of the $p\bar{p}$ atom being rapidly annihilated. The produced X-ray line width is determined by the $p\bar{p}$ annihilation from the 2p-state and is about $\Delta E \sim O(0.1 \text{ eV})$ (see the discussion and experimental measurements in [20]). As the total energy released in gamma-rays during $p\bar{H}$ annihilation is about 617 MeV (see Fig. 1), the expected fraction of X-ray line emission flux from one Pn annihilation is $f_{X,H} \approx 0.95 \times (1.7 \text{ keV}/617.5 \text{ MeV}) \approx 2.5 \times 10^{-6}$, i.e. a factor of three lower than the simple estimate given above.

3 keV X-ray emission from protonium cascades in Galactic antistar candidates

Presently, it is difficult to reliably assess the number and physical parameters of antistars in the Galaxy. Estimates in paper [10] are model-dependent and based on the assumption that gamma-ray emission from hadronic annihilation occurs in the putative antistar candidates during Bondi-Hoyle-Littleton accretion of the interstellar gas. It is straightforward to estimate the expected X-ray flux associated with the gamma-ray annihilation emission in the case where the $p\bar{p}$ annihilation was preceded by the protonium formation.

A crude estimate of the X-ray flux emitted in 1.7-keV narrow line from the gamma-ray sources – candidates to antistars found from *Fermi* 10-year LAT catalogue in ref. [18] is:

$$F_X(1.7 \text{ keV}) \sim f_{X,H} \times F_\gamma(0.1 - 100 \text{ GeV}) \approx 10^{-17} [\text{erg cm}^{-2}\text{s}^{-1}] \left(\frac{F_\gamma(0.1 - 100 \text{ GeV})}{4 \times 10^{-12} \text{ erg cm}^{-2}\text{s}^{-1}} \right) \quad (3.1)$$

(see Table 1 for individual candidates). This low flux is unlikely to be uncovered with the current instrumentation even with the stacked detection strategy.

The forthcoming JAXA/NASA XRISM (X-Ray Imaging and Spectroscopy Mission) telescope will be able to provide a 5-4 eV resolution in the 0.3-12 keV energy range [24]. The expected effective area of the *Resolve* spectrometer is $\sim 210 \text{ cm}^2$ ². For approximately 10^6 s observations, only a few 1.7-keV photons from a source with an X-ray flux of $\sim 3 \times 10^{-17} \text{ erg cm}^2 \text{ s}^{-1}$ can be collected. A more promising could be measurements from the ATHENA X-IFU X-ray spectrometer which is expected to have a spectral resolution of $\sim 2 \text{ eV}$ and an effective area of $\sim 8000 \text{ cm}^2$ in the keV range [25, 26]. The 1.7 keV Balmer line of protonium falls within the sensitivity limit of the advanced-technology Lynx X-ray Observatory [27], which will be able to measure X-ray fluxes down to $\sim 10^{-19} \text{ erg cm}^2 \text{ s}^{-1}$ with an angular resolution of better than $\sim 1''$. While the X-ray line fluxes of the individual source candidates estimated in Table 1 are below the expected sensitivity of the XRISM telescope one may try to search for antistars through stacked source detection in serendipitous surveys of the next generation X-ray observatories. In this case, the appropriate choice of the antistar candidates can be made from the unidentified *Fermi* source sample.

Note also that the most prominent 1.7-keV X-ray line from Pn decay in antistars should not interfere with other X-ray emission lines expected from stars. As no real stellar antistar counterparts have been identified inside large *Fermi* error boxes, it is reasonable to compare real *Chandra* X-ray spectra from different stars. For example, observations of solar-type dwarfs show that at energies around 2 keV only MgXII ($\lambda = 8.421 \text{ \AA} \approx 1.46 \text{ keV}$) emission is visible in spectra of young star EK Dra, the older stars demonstrating no visible emissions [28]. A giant binary nearby (about 13 pc) star

²<https://xrism.isas.jaxa.jp/research/documents/index.html>

Table 1. Estimate of possible Pn X-ray flux F_X from 4FGL *Fermi* antistar candidates. Energy flux F_γ (0.1-100) GeV from [18].

Name	F_γ (0.1 - 100 GeV) erg cm ⁻² s ⁻¹	F_X (1.7 keV) erg cm ⁻² s ⁻¹
4FGL J0548.6+1200	$(4.2 \pm 0.9) \times 10^{-12}$	$\sim 1 \times 10^{-17}$
4FGL J0948.0-3859	$(2.5 \pm 0.7) \times 10^{-12}$	$\sim 6.3 \times 10^{-18}$
4FGL J1112.0+1021	$(2.5 \pm 0.5) \times 10^{-12}$	$\sim 6.3 \times 10^{-18}$
4FGL J1232.1+5953	$(1.8 \pm 0.3) \times 10^{-12}$	$\sim 4.5 \times 10^{-18}$
4FGL J1348.5-8700	$(3.0 \pm 0.6) \times 10^{-12}$	$\sim 7.5 \times 10^{-18}$
4FGL J1710.8+1135	$(2.5 \pm 0.6) \times 10^{-12}$	$\sim 6.3 \times 10^{-18}$
4FGL J1721.4+2529	$(3.3 \pm 0.5) \times 10^{-12}$	$\sim 8.3 \times 10^{-18}$
4FGL J1756.3+0236	$(4.4 \pm 1.0) \times 10^{-12}$	$\sim 1.1 \times 10^{-17}$
4FGL J1759.0-0107	$(5.9 \pm 1.3) \times 10^{-12}$	$\sim 1.5 \times 10^{-17}$
4FGL J1806.2-1347	$(9.4 \pm 2.2) \times 10^{-12}$	$\sim 2.4 \times 10^{-17}$
4FGL J2029.1-3050	$(2.6 \pm 0.6) \times 10^{-12}$	$\sim 6.5 \times 10^{-18}$
4FGL J2047.5+4356	$(1.4 \pm 0.4) \times 10^{-11}$	$\sim 3.5 \times 10^{-17}$
4FGL J2237.6-5126	$(2.3 \pm 0.5) \times 10^{-12}$	$\sim 5.8 \times 10^{-18}$
4FGL J2330.5-2445	$(1.6 \pm 0.4) \times 10^{-12}$	$\sim 4.0 \times 10^{-18}$

Capella [29] used for the grating observations calibration [30] demonstrates a rich variety of coronal X-ray lines, with MgXII and SiXIV ($\lambda = 6.182 \text{ \AA} \approx 1.99 \text{ keV}$) around 2 keV. Therefore, the possible 1.7 keV emission from a solar-type dwarf antistar and even an evolved anti-giant is unlikely to interfere with stellar coronal X-ray lines from highly ionized species.

4 Associated e^+e^- emission and optical lines

During the formation of a Pn atom from the interaction of a proton with \bar{H} in the upper atmosphere of an antistar, a slow positron e^+ is ejected. It should form a positronium e^+e^- atom in the surrounding medium before annihilation. Since during the Pn cascade transitions and annihilation, on average, three gamma-quanta with energy $E_\gamma \approx 200 \text{ MeV}$ are created per 600 MeV (see Fig. 1), the accompanying e^+e^- annihilation flux from the *Fermi* antistar candidates is expected to be:

$$\left. \frac{dN}{dAdt} \right|_{e^+e^-} \approx 2 \times \frac{1}{3} \left. \frac{dN}{dAdt} \right|_\gamma \approx 6 \times 10^{-9} \frac{\text{ph}}{\text{cm}^2\text{s}} \left(\frac{F_\gamma(0.1 - 100 \text{ GeV})}{3 \times 10^{-12} \text{ erg cm}^{-2}\text{s}^{-1}} \right) \left(\frac{200 \text{ MeV}}{E_\gamma} \right). \quad (4.1)$$

(The factor 2 above is due to at least two photons are emitted in the Ps annihilation). This is much smaller than the current 511 keV detection capabilities [31].

Other possible traces of the Pn atom cascade decays could be searched for in the optical-UV range. Indeed, a Pn bound state is expected to be formed highly excited, $n \gtrsim 30$ [20]. The Pn energy levels are

$$E_n \approx -\frac{12.5}{n^2} \text{ keV} \approx -13.9 \text{ eV} \left(\frac{30}{n} \right)^2, \quad (4.2)$$

and the cascade transitions $(n, l = n - 1) \rightarrow (n - 1, l - 2)$ pass through the optical-UV range: $\Delta E_n \approx 0.93 \text{ eV} \left(\frac{30}{n} \right)^3$. The spacing of the optical lines is $\Delta E/E = \Delta\lambda/\lambda = 2/n$ is much larger than their expected Doppler width, which could be their distinctive feature. Clearly, the number of quanta

in an optical emission line from the *Fermi* antistar candidates should be approximately equal to the number of Pn atoms, therefore $\frac{dN}{dAdt}|_{\text{opt}} \approx \frac{dN}{dAdt}|_{\gamma} \approx 3 \times 10^{-9} \frac{\text{ph}}{\text{cm}^2\text{s}}$.

For a NIR line at $\lambda = 4\mu\text{m}$ with Doppler width $\Delta\lambda/\lambda = 3 \times 10^{-6}$ this photon flux corresponds to $m_{\text{AB}} \sim 24.3^{\text{m}}$ magnitude. While well within the rich by modern telescopes (e.g., JWST³), this flux in emission line is too small to be distinguishable on the background of stellar photons (for example, a solar-type star at a distance of 10 kpc would have $m_{\text{AB}}(4\mu\text{m}) \approx 18^{\text{m}}$ [32]). Therefore, the measurement of such weak emission lines is challenging and requires a dedicated technique (for example, the use of stellar coronagraphs to shield the stellar light, e.g. like the coronagraph to be installed on the Nancy Grace Roman Space Telescope⁴).

5 Helium-antiproton and antihelium-proton cascade X-ray lines from antistars

Enhanced production of helium and metals is an important feature of the non-standard nucleosynthesis in HBBs with high η [8–10]. Therefore, it is instructive to consider the X-ray lines arising from cascade decays of $^4\text{He}\bar{p}$ and $^4\text{He}\bar{p}$ atoms that can be created in the interaction of ISM with antistars. The possible AMS-02 detection of non-thermal antihelium-4 nuclei⁵ may indicate the presence of antistars in the Galaxy because its secondary production in the universe is challenging (see, e.g., the discussion in [33]). Note that the magnetically active antistars may accelerate antihelium nuclei in stellar flares.

In a $^4\text{He}\bar{p}$ atom, the hadronic annihilation starts dominating the cascade transitions already at the third level. The $^4\text{He}\bar{p}$ atom transitions series M (4-3) at 4.86 keV [yield $(57 \pm 3)\%$] and L (3-2) 11.13 keV [yield $(25 \pm 5)\%$] [34] are certainly of interest given that the forthcoming X-ray spectroscopic mission *XRISM* [35] is sensitive in 0.3-12 keV energy range. A simple estimate of the fractional flux in these lines relative to the annihilation gamma-ray flux can be done in the same way as for $p\bar{p}$ decays presented in the end of Section 2: $f_{\text{X,He}}(4.86\text{keV}) \approx 0.57 \times (4.86\text{ keV}/617.5\text{ MeV}) \approx 4.5 \times 10^{-6}$, $f_{\text{X,He}}(11.3\text{keV}) \approx 0.25 \times (11.3\text{ keV}/617.5\text{ MeV}) \approx 4.6 \times 10^{-6}$, i.e. about twice as high as for $p\bar{p}$ decay X-ray lines. These estimates depend on the assumed He abundance, and for the solar He abundance must be decreased accordingly. However, they are around the same as for $f_{\text{X,H}}$. These lines can be even more important from the observational viewpoint because the protonium $p\bar{p}$ 3d-2p transition line energy 1.73 keV is close to the detector's Si K-shell complex lines and, therefore, a high energy resolution is needed to distinguish the lines. Note also that in a hot medium with ionized hydrogen, when protonium atoms will not be formed, even a small mixture of He^+ ions would give rise to the effective (with atomic cross-sections) formation of $\text{He}\bar{p}$ atoms. Then only $^4\text{He}\bar{p}$ cascade X-ray lines will be produced.

A dedicated search for $^4\text{He}\bar{p}$ 4.86 keV and 11.13 keV lines in all-sky surveys like *Spectrum-RG* [36] could also constrain the collective contribution of X-ray emission from antistars with enhanced He abundance.

Like in the case of antiprotonium, $^4\text{He}\bar{p}$ atoms are formed at excited levels with principal numbers $28 < n < 35$. After an antiproton is captured, the remaining electron is rapidly ejected due to the internal Auger effect, and the process of ion $(^4\text{He}\bar{p})^+$ radiative deexcitation begins along the circular sequence from $n \sim 30$ [37]. Neglecting the strong interaction shift, the energy between consequent levels is

$$\Delta E_n \approx 3.72\text{eV} \left(\frac{30}{n} \right)^2 \frac{2n-1}{(n-1)^2}, \quad (5.1)$$

³<https://www.stsci.edu/jwst/science-planning/proposal-planning-toolbox/sensitivity-and-saturation-limits>

⁴<https://roman.gsfc.nasa.gov/coronagraph.html>

⁵S. Ting, Latest Results from the AMS Experiment on the International Space Station (2018)

Table 2. Possible cases of interaction with ISM of an antistar with velocity v and wind mass-loss rate \dot{M}_w (see text). The last column shows expected X-ray flux from Pn cascade transitions from a Galactic antistar at 1 kpc.

Velocity of antistar	Stellar wind $\dot{M}_w [M_\odot \text{ yr}^{-1}]$	Gamma-ray annihilation luminosity, $L_a [\text{erg s}^{-1}]$	Pn cascade X-ray luminosity, $L_X [\text{erg s}^{-1}]$	X-ray flux, $d = 1 \text{ kpc}$ $F_X [\text{erg cm}^{-2} \text{ s}^{-1}]$
10 km s^{-1}	≈ 0	$\sim 10^{32}$	$\lesssim 2.5 \times 10^{26}$	$\lesssim 2.5 \times 10^{-18}$
10 km s^{-1}	$\approx 10^{-10}$	$\sim 4 \times 10^{36} \dot{M}_{w,-10}$	$\lesssim 10^{31} \dot{M}_{w,-10}$	$\lesssim 10^{-13} \dot{M}_{w,-10}$
$10^{-3} c$	≈ 0	~ 0	~ 0	
$10^{-3} c$	$\approx 10^{-10}$	$\sim 4 \times 10^{36} \dot{M}_{w,-10}$	$\lesssim 10^{31} \dot{M}_{w,-10}$	$\lesssim 10^{-13} \dot{M}_{w,-10}$

and these lines can be probed in the optical range too.

6 Possible astrophysical sources

As shown above, it is challenging to test the Pn formation before hadronic annihilation in the *Fermi* Galactic antistar candidates. However, there could be favorable astrophysical conditions for the Pn creation from the interaction of hypothetical antistars with ISM.

Consider first an antistar with mass M and the standard (solar) abundance residing in the Galactic ISM with density ρ_0 (or number density n_0) and moving with the velocity v . There can be distinct cases of the star's interaction with ISM depending on the evolutionary state of the antistar (main-sequence or evolved) and its space velocity.

If the star is on the main sequence and has an insignificant mass loss via stellar wind, the interaction with ISM will be characterized by the gravitationally captured mass-rate (the Bondi-Hoyle-Littleton accretion). The relevant physical scale is the Bondi radius,

$$R_B = \frac{2GM}{(v^2 + c_s^2)} \quad (6.1)$$

where v and c_s is the star's velocity and ISM sound speed, respectively, G is the Newtonian gravitational constant. The Bondi mass accretion rate is

$$\dot{M}_B = \pi R_B^2 \rho_0 \sqrt{v^2 + c_s^2} \quad (6.2)$$

If a star has significant proper mass-loss rate \dot{M}_w , the interaction with ISM will be characterized by the radius R_w , where the dynamical pressure of the stellar wind is balanced by the ISM pressure, $\rho_w v_w^2 \sim \rho_0 c_s^2$:

$$R_w = \sqrt{\frac{\dot{M}_w (v_w / c_s)}{4\pi \rho_0 c_s}} \quad (6.3)$$

If $R_w > R_B$, the ISM accretion is insignificant and the stellar wind directly interacts with ISM. In our estimates, we will consider the standard galactic ISM with particle number density $n_0 \sim 1 \text{ cm}^{-3}$ (corresponding to a density of $\rho \sim 10^{-24} \text{ g cm}^{-3}$) and sound velocity $c_{\text{ISM}} \sim 1 \text{ km s}^{-1}$. The interaction with such an ISM depends on the stellar space velocity v and stellar wind mass-loss rate \dot{M}_w . We will consider four different cases: an antistar with or without stellar wind and typical galactic disk dispersion velocity $v \sim 10 \text{ km s}^{-1}$ or halo velocity $v \sim 10^{-3} c$ (c is the speed of light), summarized in Table 2. Note that in both cases stellar velocities are supersonic.

1. Low-velocity case, $v \sim 10 \text{ km s}^{-1}$, weak stellar wind⁶, $\dot{M}_w \approx 0$.

In this case, the Bondi radius is $R_B \approx 2 \times 10^{14} [\text{cm}] m v_6^{-2} \approx 2.7 \times 10^3 R_\odot v_6^{-2}$ (here $m \equiv (M/M_\odot)$, $v_6 \equiv v/(10^6 \text{ cm s}^{-1})$, $R_\odot \approx 7 \times 10^{10} \text{ cm}$ is the solar radius). The BHL accretion rate from ISM onto such a star is $\dot{M}_B \approx 1.8 \times 10^{11} [\text{g s}^{-1}] m^2 v_6^{-3}$. The total annihilation rate is thus $\dot{N}_a \sim 10^{35} \text{ s}^{-1}$, and the bolometric annihilation luminosity is $L_a \sim 617 \text{ MeV} \times \dot{N}_a \sim 10^{32} \text{ erg s}^{-1}$. The maximum possible Pn-cascade X-ray luminosity is then $L_X = f_{X,H} \times L_a \approx 2.5 \times 10^{26} [\text{erg s}^{-1}] m^2 v_6^{-3}$.

2. Low-velocity case, $v \sim 10 \text{ km s}^{-1}$, moderate stellar wind $\dot{M}_w \approx 10^{-10} M_\odot \text{ yr}^{-1}$. The wind terminal velocity is about the ISM sound speed, no strong shock is formed.

In this case, $R_w \approx 7 \times 10^{16} [\text{cm}] \dot{M}_{w,-10}^{1/2} n_0^{-1/2} (v_w/c_s)^{1/2} \gg R_B$. Here $\dot{M}_{w,-10} \equiv \dot{M}_w / (10^{-10} M_\odot \text{ yr}^{-1})$. The cross-section of Pn formation under these conditions is about 10^{-16} cm^2 [21]. The formation of Pn states occurs in a layer with a width of $\sim 1/(n_0 \sigma) \sim 10^{16} \text{ cm} < R_w$. The Pn formation rate is $\dot{N}_a = \dot{M}_w / m_p \sim 4 \times 10^{39} \dot{M}_{w,-10} \text{ s}^{-1}$ suggesting a bolometric annihilation gamma-ray luminosity of $L_a \sim 4 \times 10^{36} [\text{erg s}^{-1}] \dot{M}_{w,-10}$. The Pn-cascade X-ray luminosity is $L_X \lesssim 10^{31} [\text{erg s}^{-1}] \dot{M}_{w,-10}$.

3. High-velocity case, $v \sim 10^{-3} c$, weak stellar wind $\dot{M}_w \approx 0$.

This case is more relevant if antistars populate the Galactic halo and move with the halo virial velocities $v \sim 10^{-3} c$. In this case, the Bondi radius is very small, $R_B \sim 4 R_\odot v_{-3}^{-2}$ (here $v_{-3} = 10^{-3} (v/c)$), the BHL accretion is inefficient, $\dot{M}_B \sim 10^7 [\text{g s}^{-1}] m^2 n_0 v_{-3}^{-3}$, the associated annihilation luminosity is very weak.

4. High-velocity case, $v \sim 10^{-3} c$, moderate stellar wind, $\dot{M}_w \approx 10^{-10} M_\odot \text{ yr}^{-1}$.

If an antistar with stellar wind moves with the Galactic virial velocity through ISM, a strong bow shock is formed ahead of the star. The matter behind the shock front is fully ionized. The front shock radius is estimated from the dynamical wind pressure balance: $R_{sh} = \sqrt{\dot{M} v_w / (4\pi \rho_0 v^2)} \approx 7 \times 10^{16} [\text{cm}] \dot{M}_{-10}^{1/2} \rho_{-24}^{-1/2} v_{-3}^{-1/2} (v_w/v)^{1/2}$, where $\rho_{-24} = \rho / (10^{-24} \text{ g cm}^{-3})$ is the ISM density. For slow winds expected from red giants $v_w/v \sim 3 \times 10^{-5}$, and the shock radius is $R_{sh} \sim 4 \times 10^{14} [\text{cm}] \dot{M}_{-10}^{1/2} \gg R_B$.

This case is more complicated than the interaction of a cold slow stellar wind with ISM. The energy of protons downstream the shock is $E_p = (3/16) m_p v^2 \sim 170 \text{ eV}$. $\sigma \sim 10^{-23} \text{ cm}^2$ [3], and the protons penetrate much deeper into the stellar wind before annihilating through the hadronic channel. The cross-section of the Pn formation strongly depends on the proton's energy and below $\sim 1 \text{ Ry} = 13.6 \text{ eV}$ sharply increases up to a few $\times 10^{-16} \text{ cm}^2$.

However, the hot protons rapidly lose energy by interacting with neutral stellar wind. The proton stopping length in hydrogen is [M.J. Berger et al. 1993 ICRU Report 49]

$$l = \frac{E_p}{dE_p/dx} = \frac{E_p}{4\pi r_e^2 m_e c^2 \beta_p^{-2} (\rho_w/m_p) L(\beta_p)} \quad (6.4)$$

Here $\beta_p = v_p/c = 3/4 (v/c) \sim 10^{-3}$ is the proton's downstream thermal velocity, $L(\beta_p)$ is the proton's stopping number. For low proton energies, it can be evaluated only from experiments, and is dominated by nuclear scatterings. For an estimate of the stopping length of slow protons, we can use the ionization energy loss of slow protons in electron gas $L(\beta_p) \approx \log(2m_e v^2 / \hbar \omega_0)$,

⁶Solar wind mass-loss rate is $\sim 10^{-14} M_\odot$ per year.

where $\omega_0 \approx 5.6 \times 10^4 \sqrt{n_e}$ rad s⁻¹ is the electron plasma frequency [38]. For the assumed parameters, $L(\beta_p) \sim \mathcal{O}(10)$.

It is convenient to recast equation (6.4) in the form

$$l = \frac{1}{n_0 \sigma_T L(\beta_p)} \left(\frac{1}{3} \right) \left(\frac{m_p}{m_e} \right) \left(\frac{v_w}{v} \right)^2 \beta_p^4$$

($\sigma_T = (8\pi/3)r_e^2$ is the Thomson cross section). Then $l \lesssim 10^{11} [\text{cm}] (\beta_p/10^{-3})^2 (v_w/10 \text{ km s}^{-1})^2$, which is much smaller than the shock front radius $R_{sh} \sim 4 \times 10^{14} \text{ cm}$. Therefore, the ISM protons are expected to form Pn atoms inside the wind in analogy with the low-velocity case considered above.

If a typical antistar has an atmosphere like that of our Sun, then modelling by Kurucz's ATLAS code⁷ shows that the bulk of proton annihilations takes place in essentially neutral plasma. Then the data on antiproton annihilations in laboratory neutral media is quite applicable for proton annihilations in Solar-like atmospheres of antistars. Different possible atmospheric structures of antistars or their coronas deserve a special investigation.

Also note that at advanced evolutionary stages, antistars can experience a huge mass-loss, $\dot{M}_w \sim 10^{-6} M_\odot \text{ yr}^{-1}$, for a short time (e.g., at the asymptotic giant branch). In this case, as seen from Table 2, the annihilation luminosity can reach $10^{40} \text{ erg s}^{-1}$, comparable to the gamma-ray emission of the entire galaxy. Presently, this is definitely not the case in our Galaxy, but if antistars are sufficiently abundant, there can appear a bright extragalactic gamma-ray and X-ray source. Future sensitive instruments can probe this possibility.

7 Constraints from electron-positron annihilations

The interaction of an antistar with ISM should be necessarily accompanied by electron-positron annihilation. Therefore, the existing observations of the e^+e^- Galactic emission should be taken into account when constraining the possible Galactic antistar populations.

The characteristic 511 keV annihilation radiation from the Milky Way was discovered about 50 years ago in balloon-borne experiments. Since then it has been measured by many space missions (for a review, see [39, 40]). The recent analysis of *INTEGRAL SPI* Ge detector data [31] has confirmed the presence of the main extended 511 keV components with a total significance of about 58σ . The 511 keV fluxes estimations depend on the models of the extended Galactic emission. The total 511 keV flux from the Milky Way was estimated to be $(2.74 \pm 0.25) \times 10^{-3} \text{ ph cm}^{-2} \text{ s}^{-1}$. The bulge component contributed about $(0.96 \pm 0.07) \times 10^{-3} \text{ ph cm}^{-2}$, and the 511 keV flux ratio of the bulge to disk components was derived to be (0.58 ± 0.13) .

The total 511 keV Galactic disk emission suggests an annihilation flux of $F_{e^+e^-} \sim 2 \times 10^{-3} \text{ cm}^{-2} \text{ s}^{-1}$. For a fiducial distance of 10 kpc this rate corresponds to a total positron production $\dot{N}_{e^+e^-} \sim 10^{43} \text{ s}^{-1}$. If all positrons were formed in Pn $p\bar{p}$ annihilations in a purely hydrogen matter, the upper limit on the protonium production rate would be $\dot{N}_{\text{Pn}} \sim 10^{43} \text{ s}^{-1}$, corresponding to $\sim 2 \times 10^{-7} M_\odot \text{ yr}^{-1}$. Therefore, an antistar with higher wind mass-loss rate is excluded by the e^+e^- Galactic emission.

Recently, ref. [41] reported an improved *INTEGRAL* upper limit on the 511-keV flux from the Galactic satellite dwarf galaxy Ret II of $F_{511} < 1.7 \times 10^{-4} \text{ ph cm}^{-2} \text{ s}^{-1}$. Given a distance of 30 kpc to this galaxy, this flux is translated to an e^+e^- annihilation rate of about $\dot{N}_{e^+e^-} \sim 10^{43} \text{ s}^{-1}$, comparable to the detected Galactic value. The gamma-ray flux in the GeV range measured by Fermi-LAT from

⁷<http://kurucz.harvard.edu/programs.html>

Ret II galaxy is inconclusive [42]. The authors [41] do not exclude the 511 keV flux variability on a decade-long time-scale. In the frame of the astrophysical models discussed above (i.e., the interaction of antistars with ISM), the e^+e^- -flux variability might be due to the intrinsically variable stellar wind mass-loss rate.

8 Conclusions

Antistars in the universe can be created in the modified Affleck-Dine baryogenesis mechanism [4, 5]. Presently, they could be observed as old halo stars with unusual chemical composition.

In the present paper, we explored the possibility that the interaction of antistars with ISM gas can proceed with the formation of excited protonium atoms which rapidly cascade down before hadronic annihilation from 2p-states. The formation of Pn atoms most effectively occurs during the interaction of protons with neutral (or molecular) antimatter. This can happen if an antistar has a noticeable wind mass loss. We considered the case where, in analogy with ordinary stars, antistars in the mass range from ~ 0.8 to $8M_\odot$ at the end of their core nuclear burning can have cold low-velocity stellar winds $\sim 10^{-8} - 10^{-5}M_\odot \text{ yr}^{-1}$ [43, 44] (AGB antistars). The interaction of cold stellar winds from antistars with ISM can proceed through the formation of excited protonium ($p\bar{p}$) atoms. The protonium atoms cascade to the 2p-state producing mostly L (Balmer) 3d-2p X-rays around ~ 1.7 keV before the $p\bar{p}$ hadronic annihilation.

Antistars formed in HBBs should have an enhanced helium abundance. Therefore, the 4.86 keV M (4-3) and 11.13 L (3-2) narrow X-ray lines from cascade transitions in $^4\text{He}\bar{p}$ atoms can also be associated with gamma-rays from hadronic annihilations. These lines are interesting from the observational point of view because the protonium 3d-2p transition line energy 1.73 keV is close to the Si K-shell complex lines, which could hamper disentangling it from the background.

The expected Pn-decay X-ray line flux from individual Galactic *Fermi* antistar candidates reported in [18] is estimated to be much lower than the sensitivity of current X-ray detectors. However, searches for the cascade X-ray transitions from Pn and $^4\text{He}\bar{p}$ atoms associated with hadronic annihilation gamma-rays can be exciting targets for the forthcoming X-ray spectroscopic missions like *XRISM*, *Athena* and *Lynx*. Sensitive wide-field X-ray surveys can also help to constrain the collective contribution of antistars in the universe.

Acknowledgement

The authors thank the anonymous referee for careful reading of the paper and suggestions for improving the presentation of the results. We are grateful to Andrey Sokolov for help in simulating the gamma-ray spectrum from hadronic $p\bar{H}$ annihilation. The work of AD was supported by the RSF Grant 19-42-02004. SB acknowledges the support of RSF Grant 19-12-00229 in his work on stellar atmospheres. The work of KAP is supported by the Ministry of Science and Higher Education of the Russian Federation under contract 075-15-2020-778 (astrophysical appearance of antistars).

References

- [1] A. D. Sakharov, *Violation of CP Invariance, C Asymmetry, and Baryon Asymmetry of the Universe*, *Soviet Journal of Experimental and Theoretical Physics Letters* **5** (1967) 24.
- [2] A. G. Cohen, A. De Rújula and S. L. Glashow, *A Matter-Antimatter Universe?*, *ApJ* **495** (1998) 539 [[astro-ph/9707087](#)].
- [3] G. Steigman, *Observational tests of antimatter cosmologies.*, *ARAA* **14** (1976) 339.

- [4] A. Dolgov and J. Silk, *Baryon isocurvature fluctuations at small scales and baryonic dark matter*, *Physical Review D* **47** (1993) 4244.
- [5] A. D. Dolgov, M. Kawasaki and N. Kevlishvili, *Inhomogeneous baryogenesis, cosmic antimatter, and dark matter*, *Nuclear Physics B* **807** (2009) 229 [0806.2986].
- [6] S. Blinnikov, A. Dolgov, N. K. Porayko and K. Postnov, *Solving puzzles of GW150914 by primordial black holes*, *JCAP* **2016** (2016) 036 [1611.00541].
- [7] A. Dolgov and K. Postnov, *Why the mean mass of primordial black hole distribution is close to $10M_{\text{solar}}$* , *JCAP* **2020** (2020) 063 [2004.11669].
- [8] S. Matsuura, A. D. Dolgov and S. Nagataki, *Affleck-Dine Baryogenesis and Heavy Element Production from Inhomogeneous Big Bang Nucleosynthesis*, *Progress of Theoretical Physics* **112** (2004) 971 [astro-ph/0405459].
- [9] S. Matsuura, S.-I. Fujimoto, S. Nishimura, M.-A. Hashimoto and K. Sato, *Heavy element production in inhomogeneous big bang nucleosynthesis*, *Physical Review D* **72** (2005) 123505 [astro-ph/0507439].
- [10] A. Arbey, J. Auffinger and J. Silk, *Stellar signatures of inhomogeneous big bang nucleosynthesis*, *Physical Review D* **102** (2020) 023503 [2006.02446].
- [11] A. D. Dolgov, *Massive and supermassive black holes in the contemporary and early Universe and problems in cosmology and astrophysics*, *Physics Uspekhi* **61** (2018) 115 [1705.06859].
- [12] C. Bambi and A. D. Dolgov, *Antimatter in the Milky Way*, *Nuclear Physics B* **784** (2007) 132 [astro-ph/0702350].
- [13] A. D. Dolgov, V. A. Novikov and M. I. Vysotsky, *How to see an antistar*, *Soviet Journal of Experimental and Theoretical Physics Letters* **98** (2014) 519 [1309.2746].
- [14] A. D. Dolgov and S. I. Blinnikov, *Stars and black holes from the very early universe*, *Physical Review D* **89** (2014) 021301 [1309.3395].
- [15] S. I. Blinnikov, A. D. Dolgov and K. A. Postnov, *Antimatter and antistars in the Universe and in the Galaxy*, *Physical Review D* **92** (2015) 023516 [1409.5736].
- [16] P. von Ballmoos, *Antimatter in the Universe: constraints from gamma-ray astronomy*, *Hyperfine Interactions* **228** (2014) 100 [1401.7258].
- [17] J. S. Sidhu, R. J. Scherrer and G. Starkman, *Antimatter as macroscopic dark matter*, *Physics Letters B* **807** (2020) 135574 [2006.01200].
- [18] S. Dupourqué, L. Tibaldo and P. von Ballmoos, *Constraints on the antistar fraction in the Solar System neighborhood from the 10-year Fermi Large Area Telescope gamma-ray source catalog*, *Physical Review D* **103** (2021) 083016 [2103.10073].
- [19] J. Allison et al., *Geant4 developments and applications*, *IEEE Trans. Nucl. Sci.* **53** (2006) 270.
- [20] E. Klempt, F. Bradamante, A. Martin and J.-M. Richard, *Antinucleon-nucleon interaction at low energy: scattering and protonium*, *Phys. Rep.* **368** (2002) 119.
- [21] S. Y. Ovchinnikov and J. H. Macek, *Protonium formation in antiproton-hydrogen-atom collisions*, *Physical Review A* **71** (2005) 052717.
- [22] G. Reifenröther and E. Klempt, *Antiprotonic hydrogen: From atomic capture to annihilation*, *Nucl. Phys. A* **503** (1989) 885.
- [23] J. S. Cohen and N. T. Padial, *Initial distributions, cascade, and annihilation of anti-pp atoms formed in anti-p+H and anti-p+H- collisions in near vacuum*, *Physical Review A* **41** (1990) 3460.
- [24] M. Tashiro, H. Maejima, K. Toda and R. K. et al., *Concept of the X-ray Astronomy Recovery Mission*, in *Space Telescopes and Instrumentation 2018: Ultraviolet to Gamma Ray*, J.-W. A. den Herder, S. Nikzad and K. Nakazawa, eds., vol. 10699, pp. 520 – 531, International Society for Optics and Photonics, SPIE, 2018, <https://doi.org/10.1117/12.2309455>.

- [25] D. Barret, T. Lam Trong, J.-W. den Herder, L. Piro, X. Barcons, J. Huovelin et al., *The Athena X-ray Integral Field Unit (X-IFU)*, in *Space Telescopes and Instrumentation 2016: Ultraviolet to Gamma Ray*, J.-W. A. den Herder, T. Takahashi and M. Bautz, eds., vol. 9905 of *Society of Photo-Optical Instrumentation Engineers (SPIE) Conference Series*, p. 99052F, July, 2016, [1608.08105](#), [DOI](#).
- [26] D. Barret, A. Decourchelle, A. Fabian, M. Guainazzi, K. Nandra, R. Smith et al., *The Athena space X-ray observatory and the astrophysics of hot plasma*, *Astronomische Nachrichten* **341** (2020) 224 [[1912.04615](#)].
- [27] J. A. Gaskin, D. A. Swartz, A. Vikhlinin, F. Özel, K. E. Gelmis, J. W. Arenberg et al., *Lynx X-Ray Observatory: an overview*, *Journal of Astronomical Telescopes, Instruments, and Systems* **5** (2019) 021001.
- [28] P. Testa, *X-ray emission processes in stars and their immediate environment*, *Proceedings of the National Academy of Science* **107** (2010) 7158 [[1008.4343](#)].
- [29] A. J. J. Raassen and J. S. Kaastra, *X-ray variability of Capella*, *A&A* **461** (2007) 679.
- [30] F. B. S. Paerels and S. M. Kahn, *High-Resolution X-Ray Spectroscopy with CHANDRA and XMM-NEWTON*, *ARAA* **41** (2003) 291.
- [31] T. Siegert, R. Diehl, G. Khachatryan, M. G. H. Krause, F. Guglielmetti, J. Greiner et al., *Gamma-ray spectroscopy of positron annihilation in the Milky Way*, *A&A* **586** (2016) A84 [[1512.00325](#)].
- [32] C. N. A. Willmer, *The Absolute Magnitude of the Sun in Several Filters*, *ApJ Suppl. Ser.* **236** (2018) 47 [[1804.07788](#)].
- [33] V. Poulin, P. Salati, I. Cholis, M. Kamionkowski and J. Silk, *Where do the AMS-02 antihelium events come from?*, *Physical Review D* **99** (2019) 023016 [[1808.08961](#)].
- [34] M. Schneider, R. Bacher, P. Blüm, D. Gotta, K. Heitlinger, W. Kunold et al., *X-rays from antiprotonic ^3He and ^4He* , *Zeitschrift für Physik A Hadrons and Nuclei* **338** (1991) 217.
- [35] XRISM Science Team, *Science with the X-ray Imaging and Spectroscopy Mission (XRISM)*, *arXiv e-prints* (2020) arXiv:2003.04962 [[2003.04962](#)].
- [36] R. Sunyaev, V. Arefiev, V. Babyshkin, A. Bogomolov, K. Borisov, M. Buntov et al., *The SRG X-ray orbital observatory, its telescopes and first scientific results*, *A & A* **656** (2021) A132 [[2104.13267](#)].
- [37] G. Reifenröther, E. Klempt and R. Landua, *Cascade of antiprotonic helium atoms*, *Physics Letters B* **203** (1988) 9.
- [38] J. Lindgard, *On the properties of a gas of charge particles*, *Dan. Mat. Fys. Medd.* **28** (1954) .
- [39] N. Prantzos, C. Boehm, A. M. Bykov, R. Diehl, K. Ferrière, N. Guessoum et al., *The 511 keV emission from positron annihilation in the Galaxy*, *Reviews of Modern Physics* **83** (2011) 1001 [[1009.4620](#)].
- [40] E. Churazov, L. Bouchet, P. Jean, E. Jourdain, J. Knödlseider, R. Krivonos et al., *INTEGRAL results on the electron-positron annihilation radiation and X-ray & Gamma-ray diffuse emission of the Milky Way*, *New Astron. Rev.* **90** (2020) 101548.
- [41] T. Siegert, C. Boehm, F. Calore, R. Diehl, M. G. H. Krause, P. D. Serpico et al., *Reticulum II: Particle Dark Matter and Primordial Black Holes Limits*, *arXiv e-prints* (2021) arXiv:2109.03791 [[2109.03791](#)].
- [42] S. Hoof, A. Geringer-Sameth and R. Trotta, *A global analysis of dark matter signals from 27 dwarf spheroidal galaxies using 11 years of Fermi-LAT observations*, *JCAP* **2020** (2020) 012 [[1812.06986](#)].
- [43] T. Bloeker, *Stellar evolution of low and intermediate-mass stars. I. Mass loss on the AGB and its consequences for stellar evolution.*, *A&A* **297** (1995) 727.
- [44] S. Ramstedt, F. L. Schöier, H. Olofsson and A. A. Lundgren, *On the reliability of mass-loss-rate estimates for AGB stars*, *A&A* **487** (2008) 645 [[0806.0517](#)].